Determination of Lasing Material Properties using Laser Interferometry and Finite-Element Method

Xiaoyuan Peng[a], Anand Asundi[a], Yihong Chen[b], Zhengjun Xiong[b] and Gnian Cher Lim[b]

[a]*Sensors and Actuators Program, Nanyang Technological University, Nanyang Avenue, 639798*

[b]*Gintic Institute of Manufacturing Technology, 71 Nanyang Drive, 638075*

ABSTRACT

In this paper, an analytical method, which combines experimental and numerical studies, is reported to determine material properties of Nd: YVO_4. In the experimental investigation, a laser interferometer is proposed to measure the physical deformation of lasing materials. The numerical solution with the finite-element (FE) method is used to calculate distributions of temperature, stress and strain in the lasing crystal, and then Young's modulus and Poisson ratio of Nd: YVO_4 crystal are calculated to be 133GPa and 0.33, respectively.

Keywords : Nd: YVO_4 Rod, Laser Interferometer, Finite-Element Method, Mechanical properties

1. INTRODUCTION

Diode-pumped solid-state lasers offer compact, efficient, stable operation with diffraction-limited beam quality and high-power output[1-3]. Recently, a new lasing material Nd: YVO_4 applied in diode-pumped solid state (DPSS) lasers has been attracting more and more attentions due to its high efficiency[4-5]. Researchers are engaged in scaling Nd: YVO_4 lasers to high-average-power through theoretical analyses and experimental investigation[6-7]. It is a common fact that the maximum laser output power is limited by stress fracture of laser crystals, which is caused by nonuniform temperature distributions in the crystals with pump loading. The stress fracture of lasing crystals is determined by their inherent material properties. Therefore, material properties of lasing crystals, i.e., Young's modulus and Poisson ratio, are important parameters in designing and analyzing DPSS lasers. For Nd: YAG, the Young's modulus, Poisson ratio, and maximum hoop stress are 307Gpa, 0.3, and 20,000psi, respectively[8]. However, mechanical properties of Nd: YVO_4 are still unknown at present. It is, therefore, difficult to theoretically calculate the stress distribution and thermally induced birefringence effect in Nd: YVO_4, as well as predict the maximum laser output power.

In diode-end pumped solid state lasers, inhomogeneous local heating of the laser materials and nonuniform temperature distribution in lasing crystals result in distortion of the laser beam due to the temperature- and stress-dependent variation of refractive index and the pumped surface deformations[8]. Both effects contribute to the formation of a thermal lens and are referred to the thermal parts and end effect, respectively. The effect of the thermal load on the mechanical and optical

properties significantly limits the laser beam quality, resonator stability and output laser power. The end effect is in fact a kind of mechanical displacement at the end pump face. Therefore, the end physical deformation provides an essential parameter to study the properties and behaviors of the laser crystal. Precise knowledge of the thermally induced longitudinal elongation enables subsequent accurate determination of strain and stress. More importantly, as primarily measured properties, they serve as exact boundary conditions and input material data for further analytical methodologies or computational simulations using finite-element (FE) method.

It is a challenge to measure the end effect for a small size crystal (cross section of 3×3 mm^2) under actual lasing conditions. Many research efforts were focused on the thermal effects of solid state laser with the topics of measuring, modeling, and simulating thermal effects in the crystal. Koechner[8] presented roughly evaluation of the end effect for Nd: YAG, in which its end effect was less than 6% in the thermal effects. Recently, R. Weber *et al.*[9] firstly calculated and estimated the end effect of Nd: YAG rod by 2-dimensional FE analysis, and hinted that it was very difficult to separate the end effect and thermal parts by experimental methods. In other words, further quantitative verification of the end effect was practically needed to carry on.

In this paper, an analytical method, which combines experimental and numerical studies, is employed to determine material properties of Nd: YVO_4. In the experimental investigation, a laser interferometer is proposed to measure the end effect of lasing crystals. The proposed optical interferometric method provides an accurate technique for physical deformation measurements. It provides a non-invasive, high-resolution means to diagnose such effects by measuring the variations of optical path difference (OPD) by thermal loading on a lasing crystal without disturbing the normal working condition of DPSS lasers. The numerical solution with the finite-element (FE) method is used to calculate distributions of temperature, stress and strain in the lasing crystal under the same pumping condition. The boundary conditions of FE model involve the end elongation measured by the laser interferometer as an input parameter. The mechanical properties of Nd: YVO_4 crystal can be determined by the finite-element calculation. Finally, Young's modulus and Poisson ratio of Nd: YVO_4 crystal are calculated to be 133GPa and 0.33, respectively.

2. LASER INTERFEROMETRY

Figure 1 shows a schematic layout of the experimental setup of the laser interferometer used to quantify the end effect of diode-end-pumped Nd: YVO_4 lasers. A $3 \times 3 \times 5$ mm^3 Nd: YVO_4 crystal with Nd doping of 0.5 % is used as the lasing medium. It has a 1.06 μm Anti-Reflection (AR) coating at one end, and 1.06 μm high reflection (HR) coating and 808 nm anti-reflection coating at the pump end. The crystal wrapped by indium foil layer with high thermal conductivity is mounted on a copper heat sink. The crystal is end-pumped by a fiber-coupled diode laser with a central wavelength of 808 nm, and an output power ranging from 0 to 15 W. The pump beam from the fiber optics with a numerical aperture of 0.16 and diameter of 1.5 mm is focused to a spot of 600μm by a collimating and focusing optics. The lasing crystal operates at room temperature. The laser resonator consists of the HR-coated end face of Nd: YVO_4 and an output coupler with a curvature radius of 400mm and a transmission of 11%. The length of the cavity is 297 mm which results in a beam waist diameter of 600 μm at the flat mirror. With regard to the laser interferometer, a frequency stabilized He-Ne laser with a wavelength of 0.6328 μm is employed as the interferometric light source, which was split into two beams of reference beam (r) and object beam (o) by BS 1 to form the interference. M1 and M2 are two flat mirrors at the wavelength of 0.6328μm. Both BS1 and BS2 are beam splitters. A beam expander (BE) is used to magnify the interferograms. There is no disturbance on the actual

lasing operation with such an arrangement of laser interferometer because no additional optical element is required to insert in the laser resonator. The object beam is reflected from the crystal surface before interfering, therefore the interference patterns involve the surface information of the pump region on the crystal. The generated interference patterns are imaged with a CCD camera connected to a PC and a digital video recording system to allow fringe shifts to be stored for later analysis. The video system has a temporal resolution of 1/30 s.

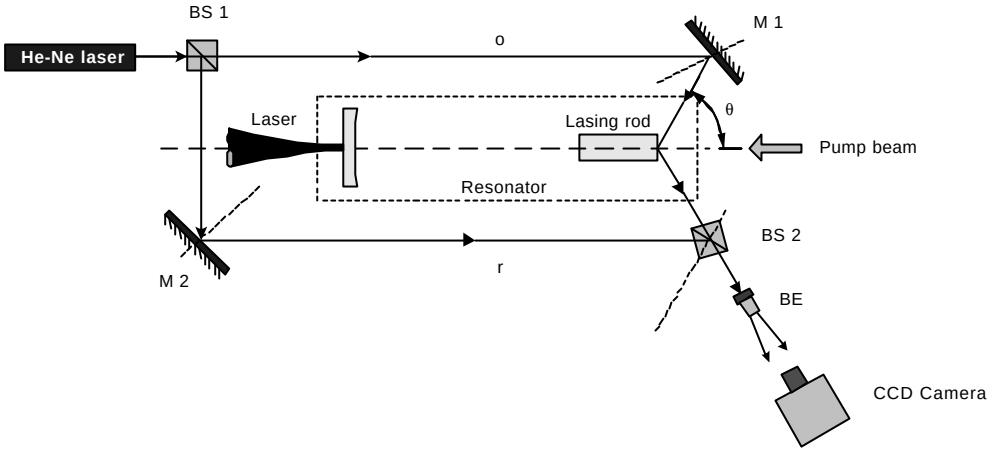

Figure 1. Schematic layout of the DPSS laser and laser interferometer

Figure 2 (a), (b), and (c) shows the fringe displacement, which is then stable for 50 seconds, and readily quantified by comparing Figure (a) with (b) and (c). The experimental procedure involves determining the number of fringe shifts as a function of the diode pump input energy. The interferograms Figure 2(a), (b), and (c) are typically taken from the different pump powers of 0 W, 5 W and 10 W, respectively.

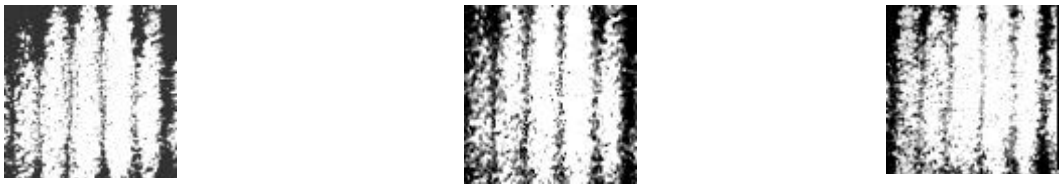

(a) (b) (c)

Figure 2. Interferograms of the end effect for an end-pumped Nd: YVO_4 crystal

The displacement of the end face together with the fixed sensitivity vectors gives the optical path differences which lead to the observable fringe patterns. In this interferometric setup, the sensitivity vectors, which define the directions of the displacement components, provide the measurement with the highest sensitivity[10]. The displacement with the nearly constant sensitivity vectors is given by

$$d_e = \frac{l\Delta f(p)}{4p\cos(q)} \tag{1}$$

where d_e is the displacement of the central point (p) of pump region; θ is the angle between the longitudinal direction and the illumination direction, in which the illumination components are setup as the same direction as the observation one; and $\Delta\phi(p)$ is the interference phase variation at point p.

Based on the Equation (1), the end elongation as a function of absorbed pump power can be calculated, which is shown in Figure 3. Taking into account the process in which fringe patterns go into stable state, interferograms under different absorbed pump power are determined after 5-second-lasing conditions.

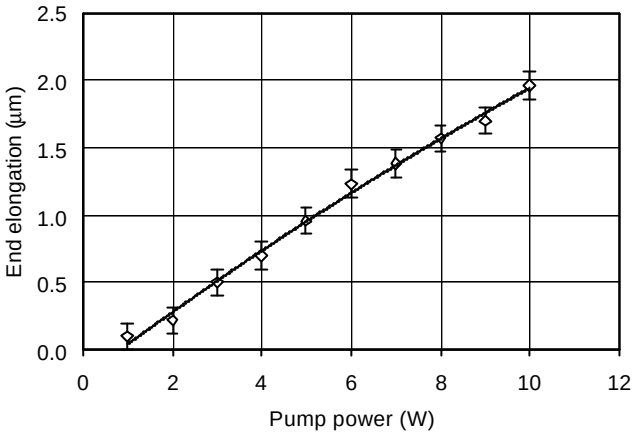

Figure 3. The end elongation as a function of pump power

It is the explicit fact that the end displacement of Nd: YVO_4 crystal becomes more serious with the increase of absorbed pump power. The end elongation of nearly 2 μm occurs on the absorbed pump power of 10 W. As a part of thermal effects, the end effect also influences the laser performance. Obviously, the end deformation makes the oscillating beam aberrated on the one hand, and causes the fracture of the crystal due to exceeding the ultimate stress on the other hand. Based on the measured physical deformation of Nd: YVO_4 crystal, together with the FEM simulating analyses, the mechanical properties of the crystal can be estimated and determined.

3. NUMERICAL MODEL AND RESULTS

A 3-D FE model, in which the one-forth part of the cuboid brick shown in Figure 4 represents the whole operation characteristic of the crystal, is presented in this paper. The numerical solution with FE method is used to calculate temperature, stress and strain distributions in the lasing crystal. The measured end deformation is served as an input parameter in FE modeling. Three kinds of material used in this model are Nd: YVO_4 crystal, copper heat sink, and indium foil, respectively. The temperature distribution T(x,y,z) is described by a three dimensional heat conduction equation[9]

$$\nabla^2 T(x, y, z) + \frac{q(x, y, z)}{k} = 0 \tag{2}$$

Where, q(x,y,z) is heat source which is the part of pump power; k is thermal conductivity.

The steady heat source, which is described as Gaussian distribution, apply heat generation rates on the crystal (heat flow rate per unit volume) as[9]

$$q(x,y,z) = h_{heat} \cdot P_0 \cdot p(x,y,z) \cdot \frac{a}{1-e^{-a \cdot L}} \cdot e^{-a \cdot z} \tag{3}$$

$$p(x,y,z) = \frac{1}{p \cdot w_p^{\,2}} \cdot e^{-\frac{2(x^2+y^2)}{w_p^{\,2}}} \tag{4}$$

$$w_p^{\,2} = w_0^{\,2}\left\{1+[\frac{l(z-z_0)}{pn_0 w_0^{\,2}}]^2\right\} \tag{5}$$

where p(x,y,z) is the normalized pump radiation distribution, P_0 is the total incident pump power, L is the doped length of the rod, α is the absorption coefficient, ω_p is the radius of pumping beam, ω_0 is the waist radius of pump beam at the position of z_0, λ is the wavelength of pumping beam, n_0 is refractive index of crystal, and η_{heat} represents the fraction of pump power converted to heat.

Here, apply temperature constraints (23 centigrade) to the periphery of heat sink as boundary condition, and insulation process on the symmetrical section. In addition, assume the boundary condition of the interface between end face and air is thermally isolated. First of all, we have to examine whether the FE model is valid to simulate the temperature distributions of crystals. Marked points in Figure 4 are selected to testify the validity of the FE model with the corresponding comparison of temperature between calculated and experimental results.

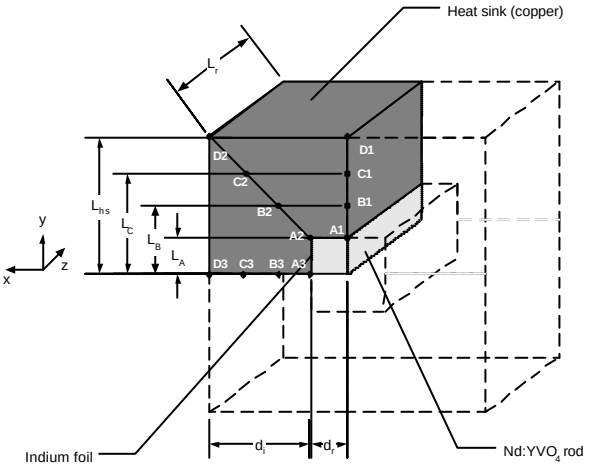

Figure 4. 3-D FE model of Nd: YVO_4 brick with copper heat sink

In Figure, L_{hs}, L_C, L_B, and L_A are set to be 5mm, 3.7mm, 2.6mm, and 1.5mm, respectively.

The temperatures at selected points shown in Table 1 are obtained by solving Equation (2) using FE analyses. By checking the numerical simulation and experimental results shown in Table 1, the deviation between calculated and measured temperature at the corresponding points is less than 2%, which shows the agreement of calculation and experiment. Therefore, the validity of the FE model is testified.

Table 1 Measured and calculated temperature values for a Nd: YVO_4 crystal

Position	A1	B1	C1	D1	A2	B2	C2	D2	A3	B3	C3	D3
Measured Temperature	27	25	24	23	26	25	24	23	27	25	24	23
FEM Temperature	27.32	24.72	24.01	23.02	26.36	24.51	23.55	23.02	27.32	24.72	24.01	23.02

The end elongation measured as a function of pump power has been obtained in Figure 3. The strain, which is served as an input parameter of FE model along the longitudinal direction, can be determined as well as a function of pump power. In order to determine the end effect of the crystal, the stress and strain are investigated by FE analyses using obtained temperature distribution. The equations of equilibrium of stresses in Cartesian coordinates are given by[11]:

$$\frac{\partial s_{xx}}{\partial x}+\frac{\partial s_{xy}}{\partial y}+\frac{\partial s_{xz}}{\partial z}=0 \tag{6}$$

$$\frac{\partial s_{yx}}{\partial x}+\frac{\partial s_{yy}}{\partial y}+\frac{\partial s_{yz}}{\partial z}=0 \tag{7}$$

$$\frac{\partial s_{xz}}{\partial x}+\frac{\partial s_{yz}}{\partial y}+\frac{\partial s_{zz}}{\partial z}=0 \tag{8}$$

where the stress components σ_{ii} represent normal components and σ_{ij}, with i not equal to j, represent shear components where the subscript i or j represents x, y, or z. In above equations, it is assumed that the shear stresses are symmetrical to exclude the case of turning moment on the crystal. This statement is expressed as $\sigma_{ij}=\sigma_{ji}$ where i here is not equal to j.

The strain-displacement relationships are defined as follows[11]:

$$e_{ij}=\frac{1}{2}\left(\frac{\partial u_i}{\partial x_j}+\frac{\partial u_j}{\partial x_i}\right) \tag{9}$$

where ε_{ii} are direct strains in the x, y and z directions, ε_{ij} with i not equal to j represent shear strains, u_i are displacements in the x, y and z directions.

According to Hooke's law, the equations relate the strain and stress components to the Young's modulus, to Poisson ration, to thermal expansion coefficient, and to local temperature expressed as[12]:

$$s_{ij}=2me_{ij}+d_{ij}\left[le-(3l+2m)aT(x,y,z)\right] \tag{10}$$

where δ_j is the Kronecher delta, T(x,y,z) is the temperature distribution inside the crystal, e is the sum of normal strains ($e=\Sigma\varepsilon_{ii}$), α is the thermal expansion coefficient, and μ are constants related to Young's modulus E and Poisson ratio ν given by:

$$l = \frac{nE}{(1+n)(1-2n)} \tag{11}$$

$$m = \frac{E}{2(1+n)} \tag{12}$$

Based on Equation (6)-(12), the stresses and strains in the crystal under prescribed temperature distributions can be simulated by using FE model. Young's modulus and Poisson ratio can be determined with the measured end deformation. The calculated temperature distributions combined with the boundary conditions are employed to fit the numerical solution with FE analyses to the measured deformation. And Young's modulus and Poisson ratio are obtained to be 133GPa and 0.33, respectively. The values of material properties are examined to be good results by simulating the end deformation with estimated Young's modulus and comparing with measured end elongation.

4. CONCLUSIONS

Material properties of lasing crystals, i.e., Young's modulus and Poisson ratio, are important parameters in designing and analyzing DPSS lasers. In this paper, an analytical method, which combines experimental and numerical studies, is employed to determine material properties of Nd: YVO_4. A laser interferometer is employed to measure the physical deformation of Nd: YVO_4 at the end pump face under lasing condition. The end elongation at the central part of pump region due to thermal expansion of the laser crystal as a function of absorbed pump power is obtained. The end effect measured here shows that the pump end face elongates nearly 2 μm with the absorbed pump power of 10W. Combined with the measured results of the end effect, the numerical solution with FE method is used to calculate distributions of temperature, stress and strain in the lasing crystal. With the testified valid FE model, the Young's modulus and Poisson ratio are finally determined to be 133GPa and 0.33, respectively.

REFERENCE

1. T. Y. Fan, and R. L. Byer, " Diode laser pumped solid-state lasers", *IEEE J. of Quantum Electronics*, 24 (8), pp. 895-912, 1988.

2. S. C. Tidwell, J. F. Seamans, C. E. Hamilton, C. H. Muller, and D. D. Lowenthal, " Efficient, 15W output power, diode-end-pumped Nd: YAG laser", *Optics Letters*, 16 (8), pp. 584-586, 1991.

3. D. Golla, M. Bode, S. Knoke, W. Schone, G. Ernst, and A. Tunnermann, "62-W CW TEM_{00} Nd:YAG laser side-pumped by fiber-coupled diode lasers", *Optics Letters*, 21 (3), pp. 201-212, 1996.

4. W. L. Nighan, D. Dudley, and M. S. Keirstead, "Diode-bar-pumped Nd:YVO_4 lasers with > 13W TEM_{00} output at > 50% efficiency", *OSA Tech. Dig. Series*, pp. 17-18, 1995.

5. J. Zhang, M. Quade, K. M. Du, Y. Liao, S. Falter, M. Baumann, P. Loosen, and R. Poprawe, " Efficient TEM_{00} operation of Nd:YVO_4 laser and end pumped by fiber-coupled diode laser",*Electronic Letters*, 33 (9), pp. 775-777, 1997.

6. Y. F. Chen, " Design criteria for concentration optimization in scaling diode end-pumped lasers to high powers: Influence of thermal fracture",*IEEE Quantum Electronics*, 35(2), pp. 234-239, 1999.

7. M. Tsunekane, N. Taguchi, T. Kaamatsu, and H. Inaba, "Analytical and experimantal studies on the characteristics of composite solid-state laser rods in diode-end-pumped geometry", *IEEE J. Selected Topics in Quantum Electronics*, 3 (1), pp. 9-19, 1997.

8. W. Koechner, *Solid-state Laser Engineering (Third Edition)*, Spronger-Verlag, USA, pp. 388-392, 1992.

9. R. Weber, B. Neuenschwander, M. Macdonald, M. B. Roos, and H. P. Weber, " Cooling schemes for longitudinally diode laser-pumped Nd: YAG rods", *IEEE J. of Quantum Electronics*, 34 (6), pp. 1046-1053, 1998.

10. T. Kreis, *Holographic Interferometry Principles and Methods*, Akademie Verlag GmbH, Berlin, pp. 78-82, 1996.

11. A. A. Becker, *The Boundary Element Method in Engineering*, McGraw-Hill Book Co., UK, 1992.

12. B. A. Boley, and J. H. Weiner, *Theory of Thermal Stresses*, John Wiley & Sons, Inc., New York, 1960.